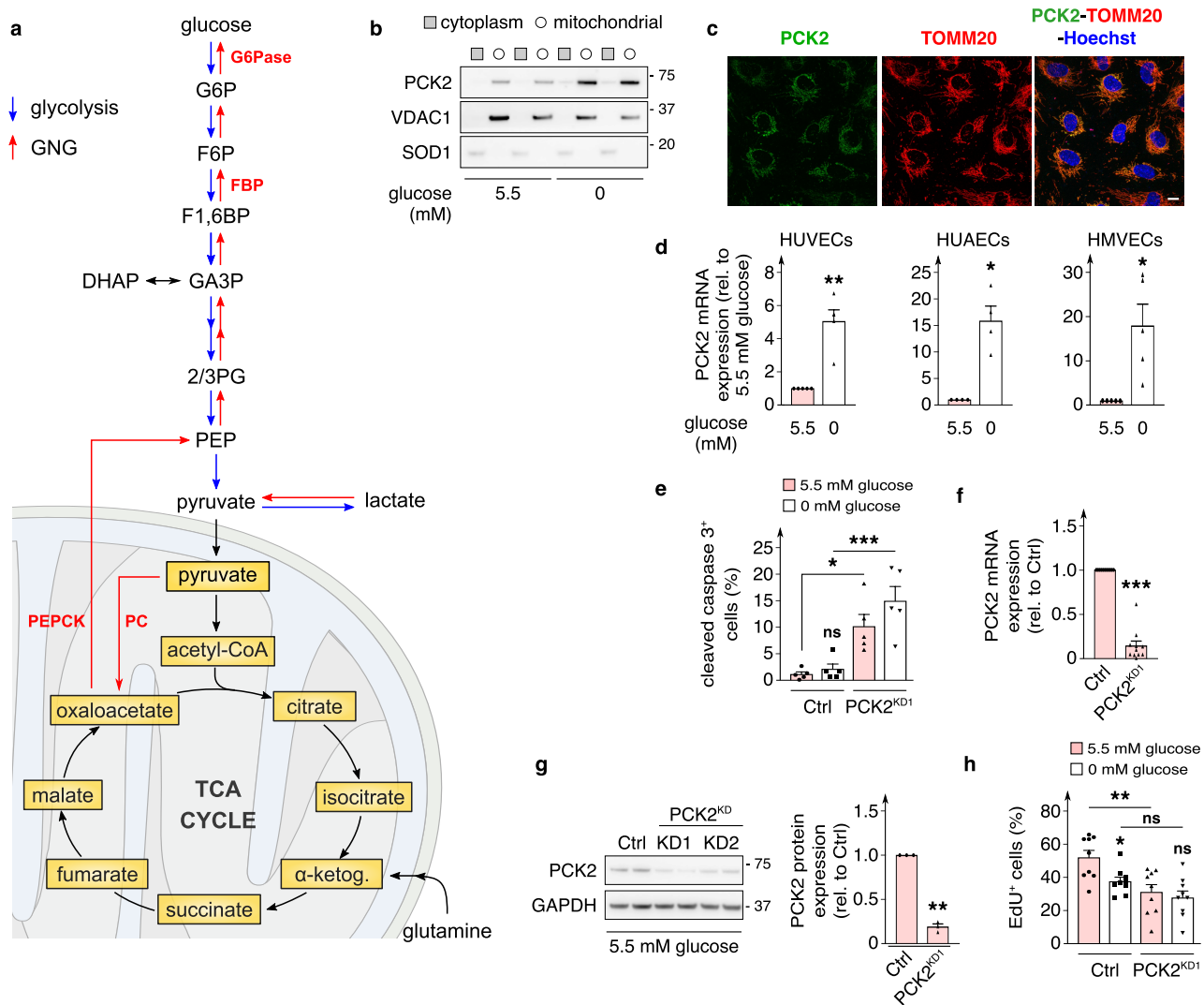


SUPPLEMENTARY INFORMATION

- SUPPLEMENTARY FIGURES
- SUPPLEMENTARY DATA 1 (LEGEND)

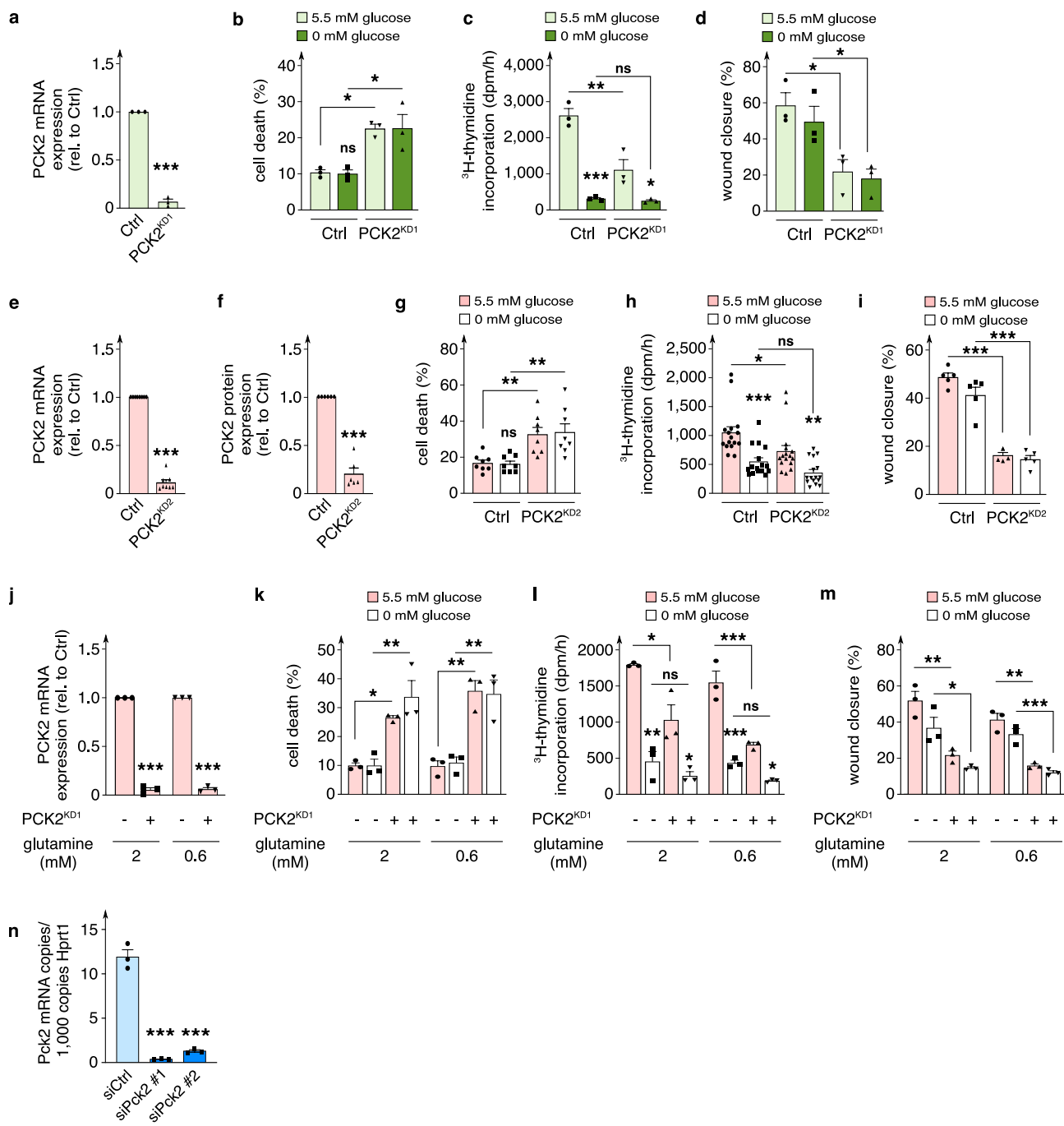
Figure S1



SUPPLEMENTARY FIGURE 1: ROLE OF ENDOTHELIAL PCK2 IN VESSEL SPROUTING

a, Graphical representation of the gluconeogenic (GNG) and glycolytic pathway with indication of the key rate-controlling GNG enzymes glucose-6-phosphatase (G6Pase), fructose-1,6-bisphosphatase (FBP), phosphoenol-pyruvate (PEP) carboxykinase (PEPCK, also termed PCK) and pyruvate carboxylase (PC). Other abbreviations (from top to bottom): G6P, glucose-6-phosphate; F6P, fructose-6-phosphate; F1,6BP, fructose-1,6-bisphosphate; GA3P, glyceraldehyde-3-phosphate; DHAP, dihydroxyacetone phosphate; 2/3PG, 2/3-phosphoglycerate; α -ketog., α -ketoglutarate; TCA cycle, tricarboxylic acid cycle. **b**, Representative immunoblot of PCK2 protein levels in mitochondrial and cytoplasmic fractions of ECs cultured in 5.5 *versus* 0 mM glucose (n=3). VDAC1 is used as a mitochondrial marker; SOD1 is used as a cytoplasmic marker. Squares: cytoplasm; circles: mitochondrial. **c**, Representative immunofluorescence images of PCK2 (green), TOMM20 (red; mitochondrial marker) and Hoechst (blue; nucleus marker) staining in ECs cultured in 5.5 mM glucose (scale bar represents 10 μ m) (representative for n=3 independent experiments). **d**, qRT-PCR analysis of *PCK2* mRNA level in human venous ECs (HUVECs; n=5), arterial ECs (HUAECs; n=4) and microvascular ECs (HMVECs; n=5) cultured for 48 hours in 5.5 *versus* 0 mM glucose (data expressed relative to 5.5 mM glucose). **e**, Quantification of apoptotic cleaved caspase 3⁺ in control and PCK2^{KD1} ECs in 5.5 *versus* 0 mM glucose (n=5). **f**, qRT-PCR analysis of *PCK2* mRNA level in control and PCK2^{KD1} ECs in 5.5 mM glucose (data expressed relative to control (Ctrl)) (n=11). **g**, Representative immunoblot and densitometric quantification of PCK2 protein level in Ctrl, PCK2^{KD1} (n=3) and PCK2^{KD2} (n=6) ECs in 5.5 mM glucose (densitometric data relative to Ctrl). GAPDH was used as a loading control. **h**, EdU incorporation into DNA in control and PCK2^{KD1} ECs in 5.5 *versus* 0 mM glucose (n=9). Data are mean \pm s.e.m. Statistics: one-sample t-test (**d,f,g**), ANOVA (**e,h**); * $P < 0.05$; ** $P < 0.01$; *** $P < 0.001$; ns, not significant.

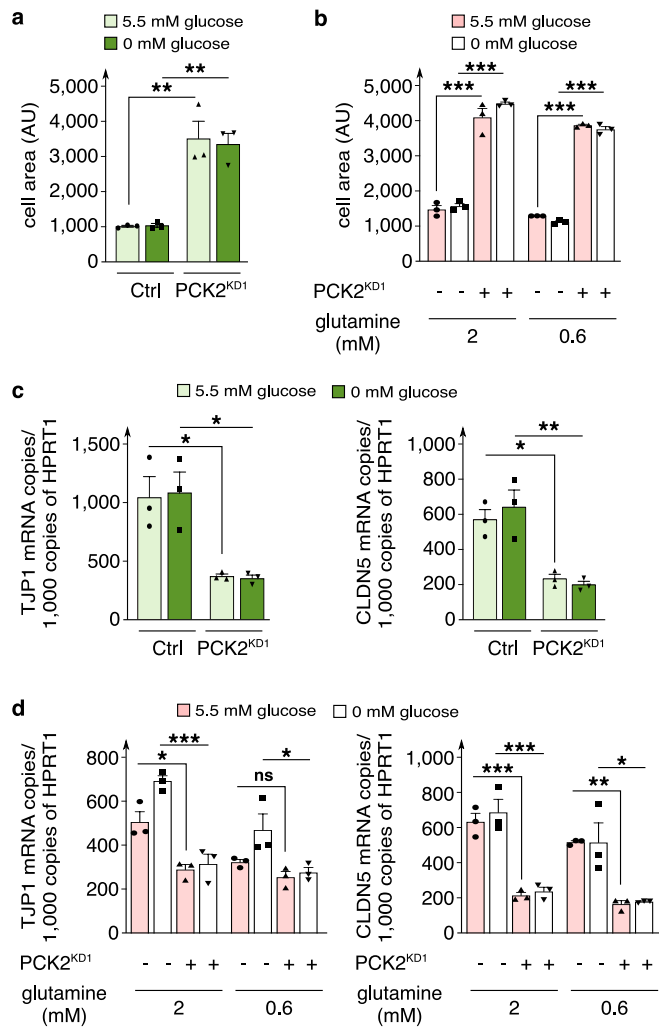
Figure S2



SUPPLEMENTARY FIGURE 2: SILENCING OF *PCK2* IN DIFFERENT EC TYPES AND CONDITIONS

a, qRT-PCR analysis of *PCK2* mRNA level in control and PCK2^{KD1} HUAECs in 5.5 mM glucose (data expressed relative to control (Ctrl)) (n=3). **b,c**, Cell death (**b**) and ³H-thymidine incorporation into DNA (**c**) in control and PCK2^{KD1} HUAECs in 5.5 *versus* 0 mM glucose (n=3). **d**, Scratch wound closure in MitoC-treated control and PCK2^{KD1} HUAECs in 5.5 *versus* 0 mM glucose (n=3). **e**, qRT-PCR analysis of *PCK2* mRNA level in control and PCK2^{KD2} ECs in 5.5 mM glucose (data expressed relative to control (Ctrl)) (n=8). **f**, Densitometric quantification of PCK2 protein level in Ctrl and PCK2^{KD2} ECs in 5.5 mM glucose (densitometric data relative to Ctrl) (n=6). See also representative immunoblot in Supplementary Figure 1g. **g,h**, Cell death (**g**; n=8) and ³H-thymidine incorporation into DNA (**h**; n=16) in control and PCK2^{KD2} ECs in 5.5 *versus* 0 mM glucose. **i**, Scratch wound closure in MitoC-treated control and PCK2^{KD2} ECs in 5.5 *versus* 0 mM glucose (n=5). **j**, qRT-PCR analysis of *PCK2* mRNA level in control and PCK2^{KD1} ECs in 5.5 mM glucose in lower glutamine concentrations (2 or 0.6 mM; data expressed relative to control (Ctrl)) (n=3). **k,l**, Cell death (**k**) and ³H-thymidine incorporation into DNA (**l**) in control and PCK2^{KD1} ECs in 5.5 *versus* 0 mM glucose in lower glutamine concentrations (2 or 0.6 mM) (n=3). **m**, Scratch wound closure in MitoC-treated control and PCK2^{KD1} ECs in 5.5 *versus* 0 mM glucose in lower glutamine concentrations (2 or 0.6 mM) (n=3). **n**, qRT-PCR analysis of *Pck2* mRNA level in murine E2 ECs transfected with negative control siRNA (siCtrl) or siRNAs against murine *Pck2*, expressed relative to the *Hprt1* housekeeping gene (n=3). Data are mean ± s.e.m. Statistics: one-sample t-test (**a,e,f,j**), ANOVA (**b-d,g-l,k-n**); * *P* < 0.05; ** *P* < 0.01; *** *P* < 0.001; ns, not significant. dpm, disintegrations per minute.

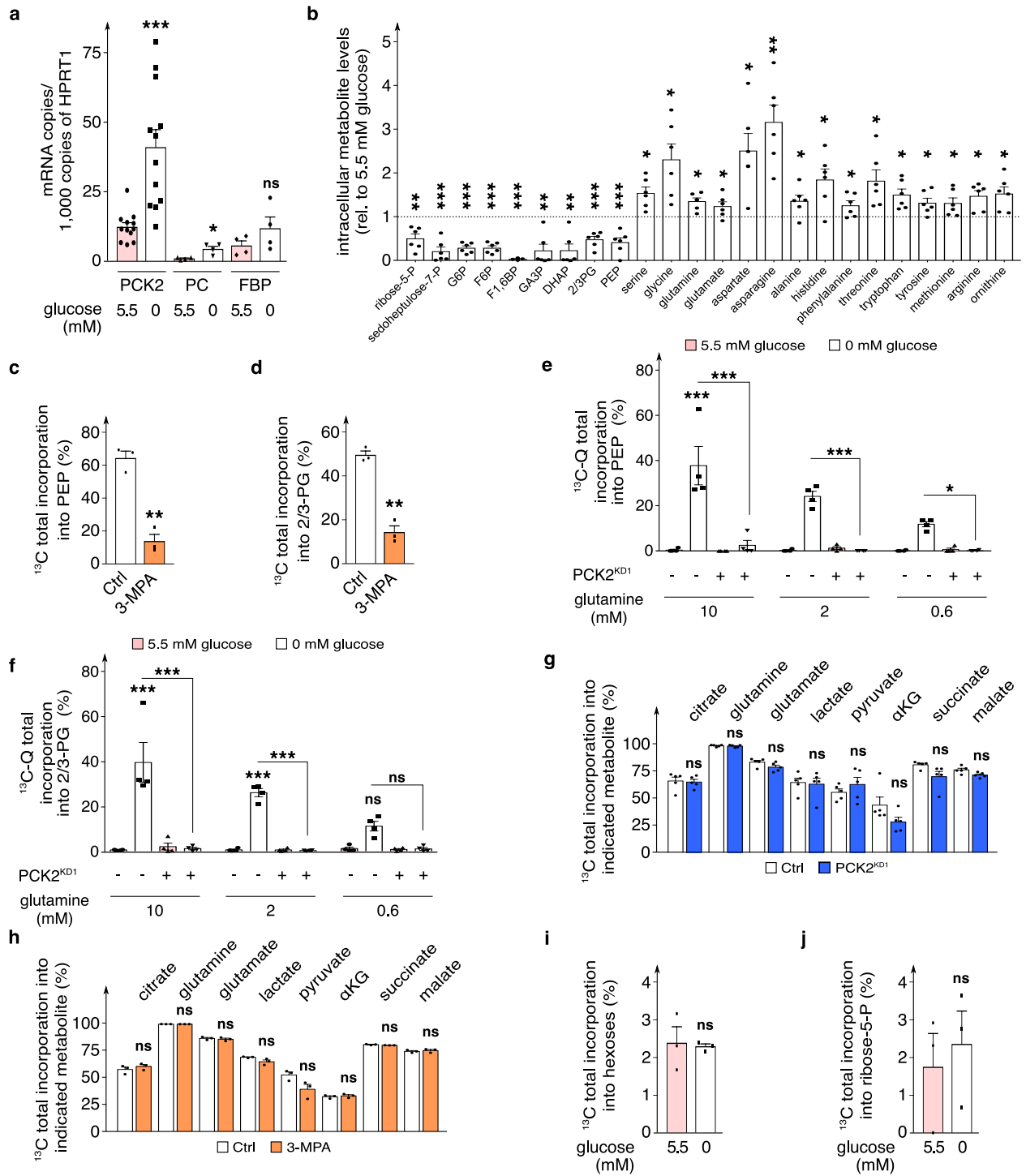
Figure S3



SUPPLEMENTARY FIGURE 3: EFFECT OF PCK2 SILENCING ON EC MORPHOLOGY AND MEMBRANE INTEGRITY

a, Quantification of cell area in control and PCK2^{KD1} HUAECs in 5.5 *versus* 0 mM glucose (n=3). **b**, Quantification of cell area in control and PCK2^{KD1} ECs in 5.5 *versus* 0 mM glucose in lower glutamine concentrations (2 or 0.6 mM) (n=3). **c**, qRT-PCR analysis of tight junction protein 1 (*TJP1*) and claudin-5 (*CLDN5*) mRNA levels in control and PCK2^{KD1} HUAECs in 5.5 *versus* 0 mM glucose (n=3). **d**, qRT-PCR analysis of tight junction protein 1 (*TJP1*) and claudin-5 (*CLDN5*) mRNA levels in control and PCK2^{KD1} ECs in 5.5 *versus* 0 mM glucose in lower glutamine concentrations (2 or 0.6 mM) (n=3). Data are mean \pm s.e.m. Statistics: ANOVA (**a-d**); * $P < 0.05$; ** $P < 0.01$; *** $P < 0.001$; ns, not significant. AU, arbitrary units.

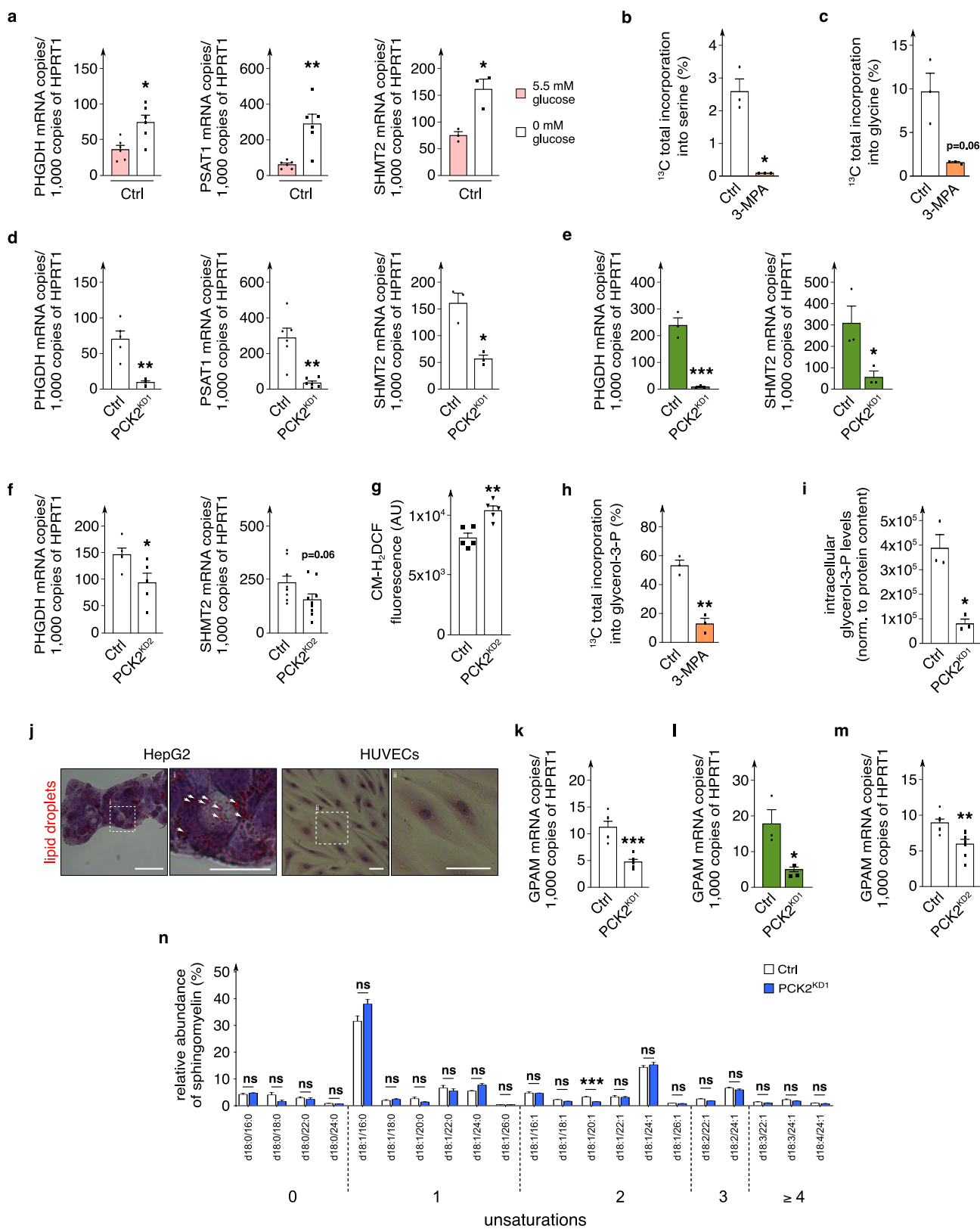
Figure S4



SUPPLEMENTARY FIGURE 4: PCK2 CONTROLS CHANNELING OF GLUTAMINE- AND LACTATE-DERIVED CARBONS INTO LOWER GLYCOLYTIC INTERMEDIATES IN GLUCOSE-DEPRIVED ECTS

a, qRT-PCR analysis of *PCK2* (n=12), *PC* (n=4) and *FBP* (n=4) mRNA levels in ECTS cultured in 5.5 *versus* 0 mM glucose. **b**, Intracellular levels of pentose phosphate pathway metabolites (ribose-5-phosphate and sedoheptulose-7-phosphate), glycolytic intermediates and amino acids in glucose-deprived ECTS (relative to control 5.5 mM glucose ECTS; represented by the dotted line) (n=6). **c,d**, Incorporation of [^{13}C]-glutamine and [^{13}C]-lactate carbon into total intracellular PEP pool (**c**) and 2/3-PG pool (**d**) in control and 3-mercaptopicolinic acid (3-MPA; 100 μM , 48 hour)-treated glucose-deprived ECTS (n=3). **e,f**, Incorporation of [^{13}C]-glutamine carbon into total intracellular phosphoenolpyruvate (PEP) pool (**e**) and 2/3-phosphoglycerate (2/3-PG) pool (**f**) in control and *PCK2*^{KD1} ECTS in 5.5 *versus* 0 mM glucose in different glutamine concentrations (10, 2 or 0.6 mM) (n=3). **g,h**, Incorporation of [^{13}C]-glutamine and [^{13}C]-lactate carbon into total intracellular pool of metabolites downstream of PEP (including TCA cycle intermediates) in control and *PCK2*^{KD1} (**g**; n=5) or 3-MPA-treated (**h**; n=3) glucose-deprived ECTS. **i,j**, Incorporation of [^{13}C]-glutamine and [^{13}C]-lactate carbon into total intracellular hexoses (fructose-6-phosphate (F6P) and glucose-6-phosphate (G6P)) pool (**i**) and ribose-5-phosphate pool (**j**) in ECTS in 5.5 *versus* 0 mM glucose (n=3). Data are mean \pm s.e.m. Statistics: two-tailed t-test with Welch's correction (**a,c,d,g-j**), ANOVA (**e,f**), one-sample t-test (**b**); * $P < 0.05$; ** $P < 0.01$; *** $P < 0.001$; ns, not significant. αKG , α -ketoglutarate.

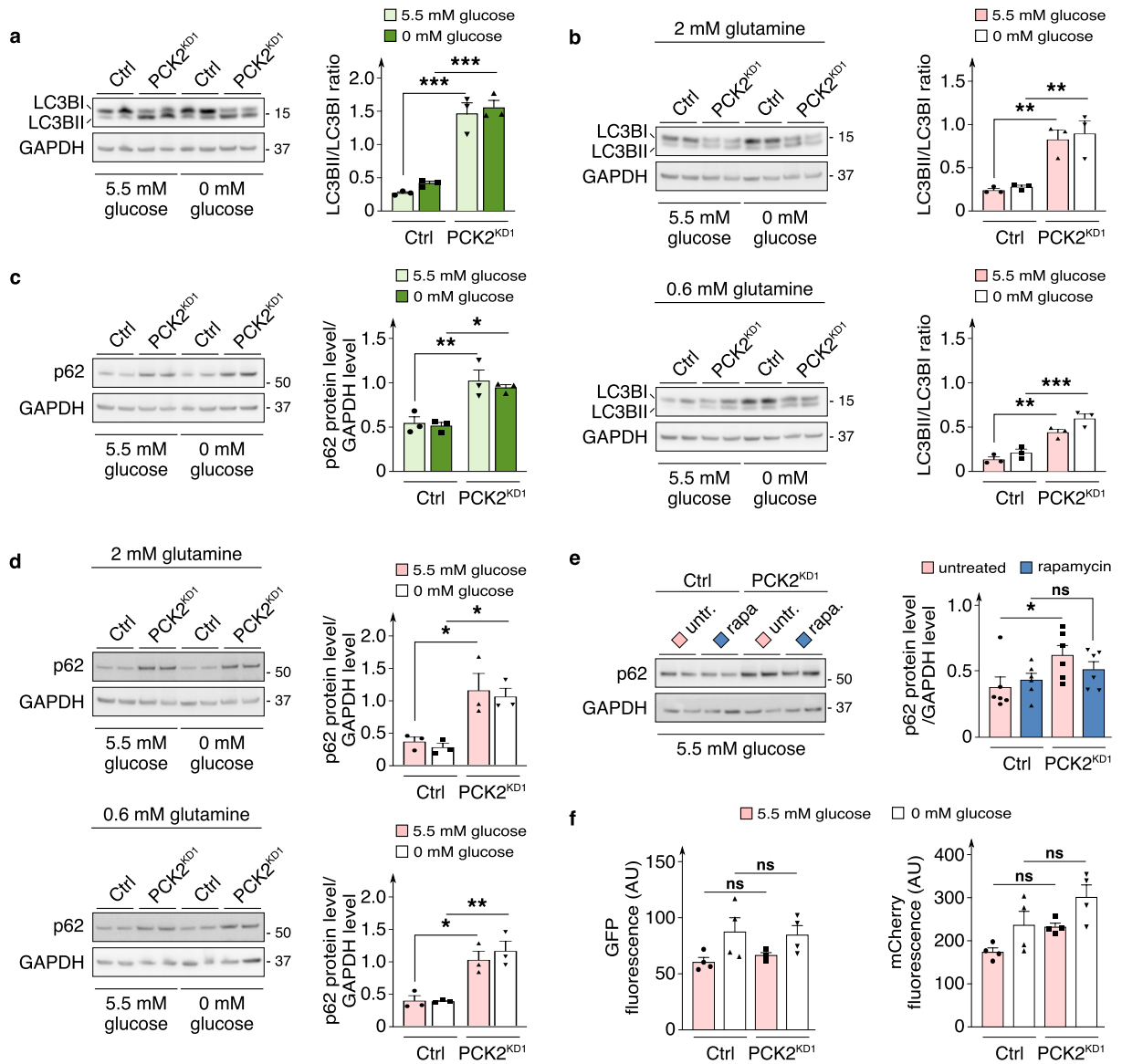
Figure S5



SUPPLEMENTARY FIGURE 5: PCK2-DERIVED GLYCOLYTIC INTERMEDIATES SHUTTLE INTO SERINE/GLYCINE BIOSYNTHESIS AND GLYCERONEOGENESIS

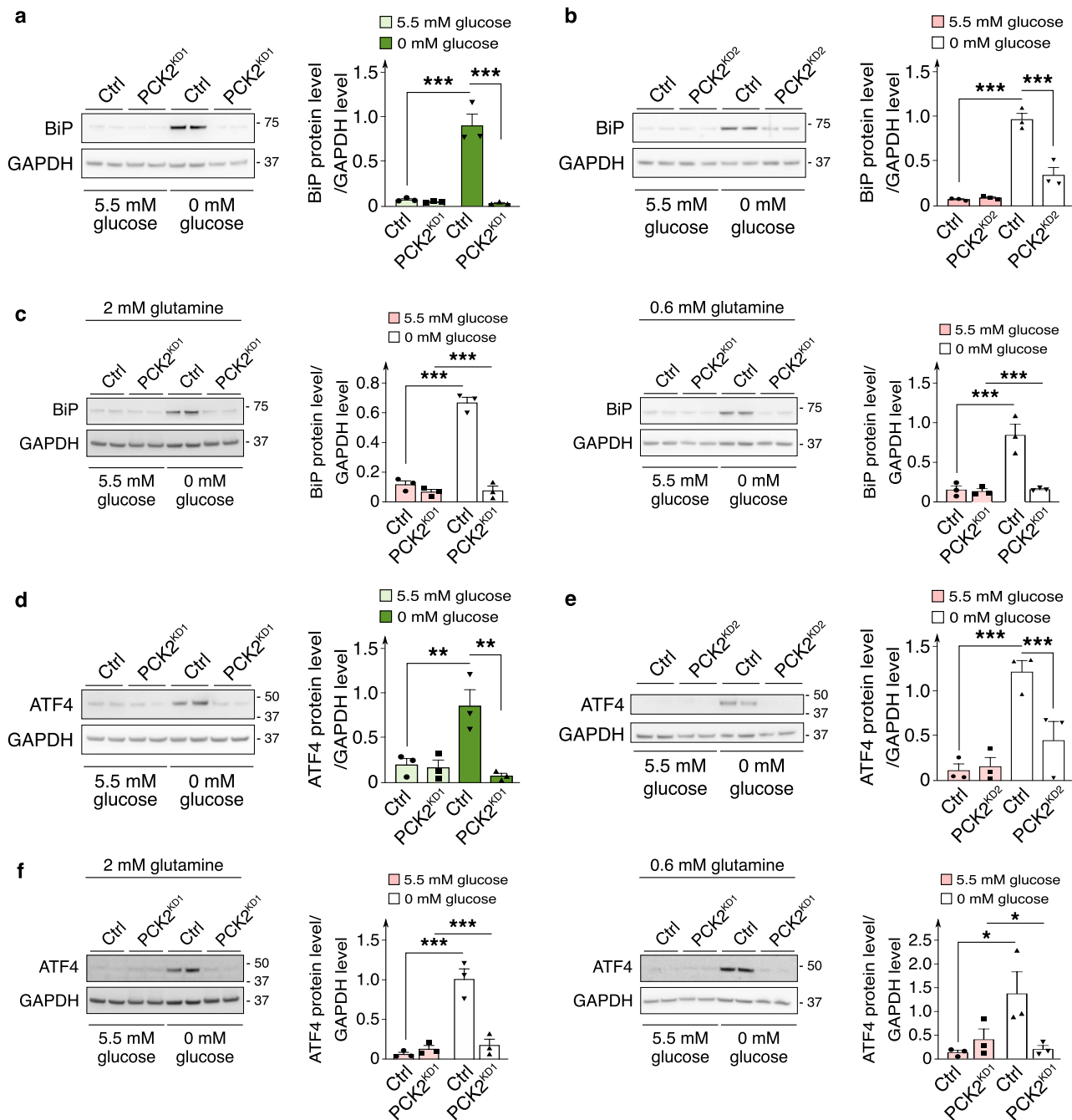
a, qRT-PCR analysis of *PHGDH* (n=6), *PSAT1* (n=6) and *SHMT2* (n=3) mRNA levels in ECs cultured in 5.5 versus 0 mM glucose. **b,c**, Incorporation of [¹³C]-glutamine and [¹³C]-lactate carbon into total intracellular serine pool (**b**) and glycine pool (**c**) in control or 3-MPA-treated glucose-deprived ECs (n=3). **d-f**, qRT-PCR analysis of mRNA levels of genes involved in serine and glycine biosynthesis pathway in control and PCK2^{KD1} glucose-deprived ECs (**d**; *PHGDH*, n=6; *PSAT1*, n=6; *SHMT2*, n=3), in control and PCK2^{KD1} glucose-deprived HUAECs (**e**; *PHGDH*, n=3; *SHMT2*, n=3), or in control and PCK2^{KD2} glucose-deprived ECs (**f**; *PHGDH*, n=5; *SHMT2*, n=9). **g**, Quantification of cellular ROS levels (measured as median CM-H₂DCF fluorescence levels) in control and PCK2^{KD2} glucose-deprived ECs (n=3). **h**, Incorporation of [¹³C]-glutamine and [¹³C]-lactate carbon into total intracellular glycerol-3-phosphate pool in control and 3-MPA-treated glucose-deprived ECs (n=3). **i**, Intracellular levels of glycerol-3-phosphate, normalized (norm.) to protein content (expressed in AUC/μg protein), in control and PCK2^{KD1} glucose-deprived ECs (n=3). **j**, Representative images of lipid droplet staining in HepG2 cells (used as positive control) and HUVECs. For both cell types, the panels to the right are magnifications of the respective boxed area indicated in the left panel (scale bars represent 50 μm in the original left panels, 25 μm in the magnifications). White arrowheads denote the presence of lipid droplets (red) (representative for n=3 independent experiments). **k-m**, qRT-PCR analysis of *GPAM* mRNA levels in control and PCK2^{KD1} glucose-deprived ECs (**k**; n=6), in control and PCK2^{KD1} glucose-deprived HUAECs (**l**; n=3), or in control and PCK2^{KD2} glucose-deprived ECs (**m**; n=7). **n**, Phospholipidomic profile analysis showing the relative abundance of saturated, mono-, di- and poly-unsaturated sphingomyelin lipid species in control or PCK2^{KD1} glucose-deprived ECs (n=4). The numbers under the bars indicate the carbon length of the fatty acid for the different sphingomyelin lipid species within each group of unsaturation degree (zero to ≥ 4). Data are mean ± s.e.m. Statistics: two-tailed t-test with Welch's correction (**a-i,k-n**); * *P* < 0.05; ** *P* < 0.01; *** *P* < 0.001; ns, not significant. AU, arbitrary units.

Figure S6



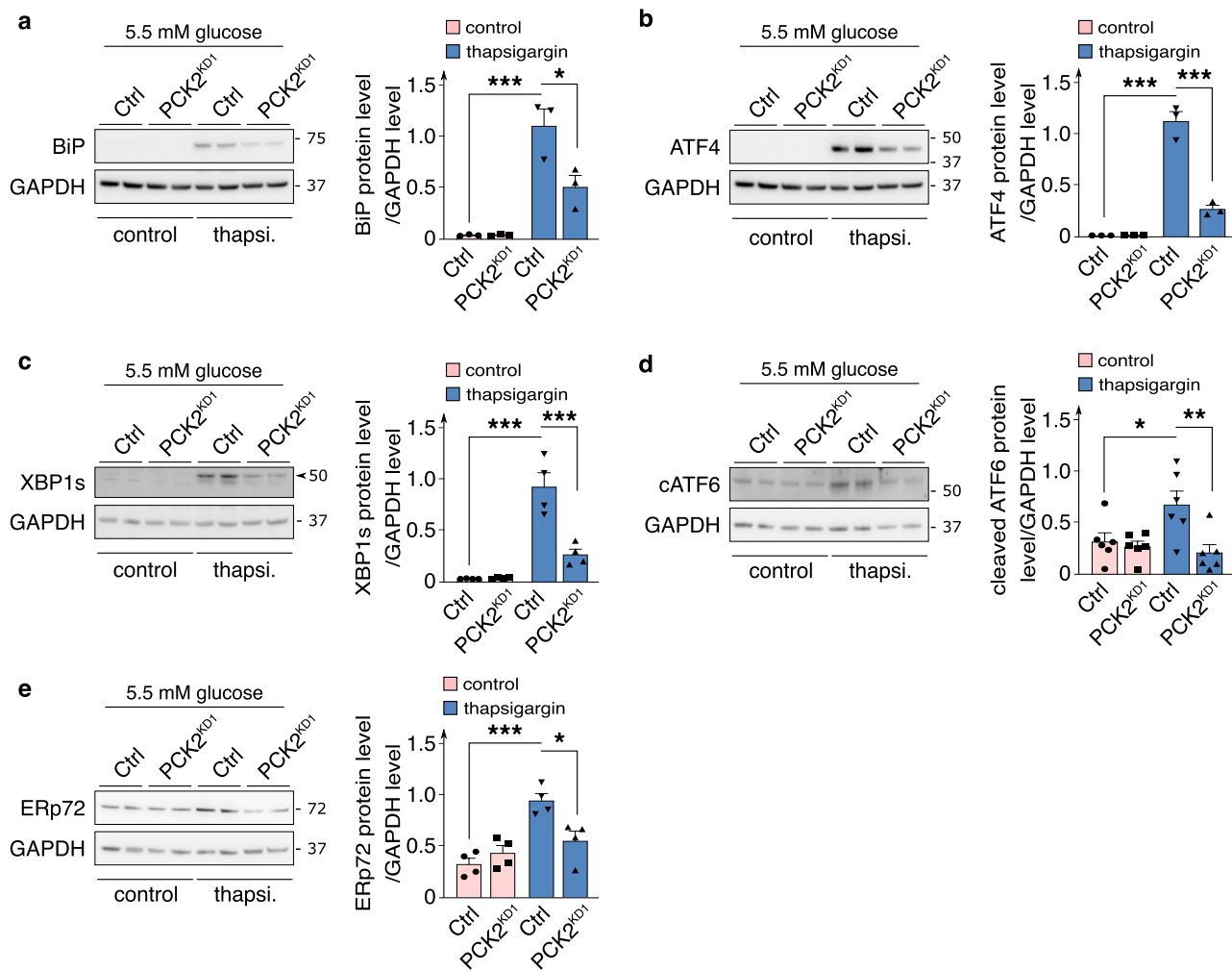
SUPPLEMENTARY FIGURE 6: PCK2-SILENCED Ecs HAVE DECELERATED AUTOLYSOSOMAL CLEARANCE OF PROTEIN AGGREGATES

a,b, Representative immunoblot of LC3B protein level and densitometric quantification of LC3BII (lipidated)/LC3BI (non-lipidated) ratio in control and PCK2^{KD1} HUAECs in 5.5 *versus* 0 mM glucose (**a**; n=3) or in control and PCK2^{KD1} ECs in 5.5 *versus* 0 mM glucose in lower glutamine concentrations (2 or 0.6 mM) (**b**; n=3). GAPDH was used as a loading control. **c,d**, Representative immunoblot and densitometric quantification of p62 protein level in control and PCK2^{KD1} HUAECs in 5.5 *versus* 0 mM glucose (**c**; n=3) or in control and PCK2^{KD1} ECs in 5.5 *versus* 0 mM glucose in lower glutamine concentrations (2 or 0.6 mM) (**d**; n=3). GAPDH was used as a loading control. Immunoblotting for p62 in ECs was done on the same blot as the LC3BI/II immunoblotting of panel b (see above), hence the same GAPDH loading control is shown in both panels. **e**, Representative immunoblot and densitometric quantification of p62 protein levels in control and PCK2^{KD1} ECs in 5.5 mM glucose with 24-hour 50 nM rapamycin (rapa.) or without treatment (untr.) (n=6). **f**, Quantification of median GFP and mCherry fluorescence levels in control and PCK2^{KD1} ECs overexpressing mCherry(acid-insensitive)-GFP(acid-sensitive)-LC3 (see Methods) in 5.5 *versus* 0 mM glucose (n=4). Data are mean \pm s.e.m. Statistics: ANOVA (**a-f**); * $P < 0.05$; ** $P < 0.01$; *** $P < 0.001$; ns, not significant. AU, arbitrary units.

Figure S7

SUPPLEMENTARY FIGURE 7: EFFECT OF PCK2 SILENCING ON PROTEOSTASIS IN GLUCOSE-DEPRIVED ECS

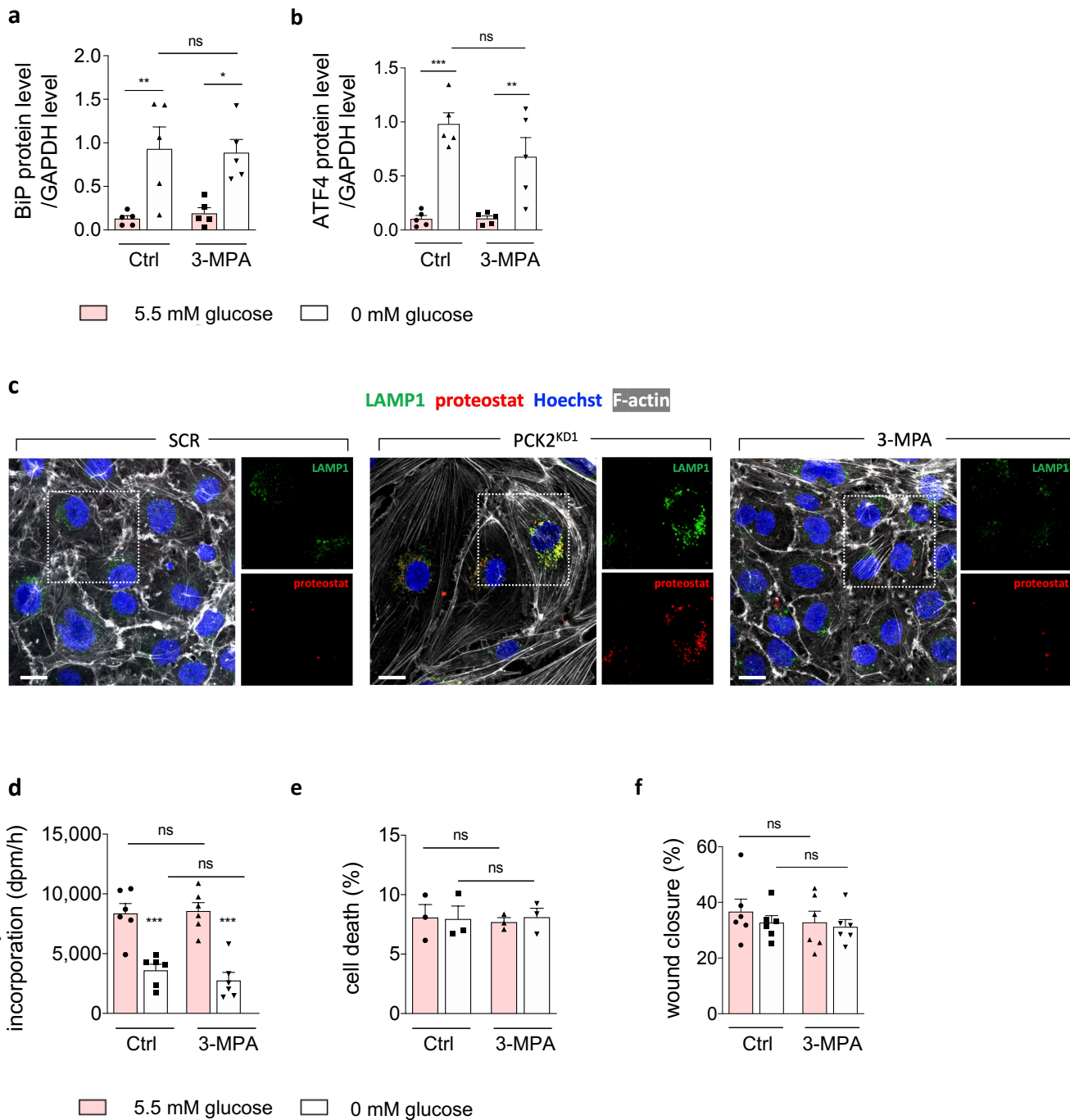
a-c Representative immunoblot and densitometric quantification of BiP protein levels in control and PCK2^{KD1} HUAECs in 5.5 *versus* 0 mM glucose (**a**; n=3), in control and PCK2^{KD2} ECs in 5.5 *versus* 0 mM glucose (**b**; n=3), or in control and PCK2^{KD1} ECs in 5.5 *versus* 0 mM glucose in lower glutamine concentrations (2 or 0.6 mM) (**c**; n=3). GAPDH was used as a loading control. **d-f** Representative immunoblot and densitometric quantification of ATF4 protein levels in control and PCK2^{KD1} HUAECs in 5.5 *versus* 0 mM glucose (**d**; n=3), in control and PCK2^{KD2} ECs in 5.5 *versus* 0 mM glucose (**e**; n=3), or in control and PCK2^{KD1} ECs in 5.5 *versus* 0 mM glucose in lower glutamine concentrations (2 or 0.6 mM) (**f**; n=3). GAPDH was used as a loading control. Immunoblotting of ECs in f (2 mM glutamine condition) was done on the same blot as the BiP immunoblotting of panel c (2 mM condition) (see above), hence the same GAPDH loading control is shown in both panels. Data are mean \pm s.e.m. Statistics: ANOVA (**a-f**); * $P < 0.05$; ** $P < 0.01$; *** $P < 0.001$; ns, not significant.

Figure S8

SUPPLEMENTARY FIGURE 8: EFFECT OF PCK2 SILENCING ON PROTEOSTASIS IN NORMAL GLUCOSE ECS UPON TREATMENT WITH ER STRESSOR (THAPSIGARGIN)

a-e, Representative immunoblot and densitometric quantification of BiP (**a**; n=3), ATF4 (**b**; n=3), spliced XBP1 (XBP1s; see black arrowhead) (**c**; n=4), cleaved ATF6 (cATF6) (**d**; n=6) and ERp72 (**e**; n=4) protein levels in control and PCK2^{KD1} ECs in 5.5 mM glucose with 6-hour 2 μ M thapsigargin (thapsi.) or without treatment (control). GAPDH was used as a loading control. Immunoblotting for ATF4 (panel b) was done on the same blot as the immunoblotting of BiP (panel a), hence the same GAPDH loading control is shown in both panels. Data are mean \pm s.e.m. Statistics: ANOVA (**a-e**); * $P < 0.05$; ** $P < 0.01$; *** $P < 0.001$.

Figure S9

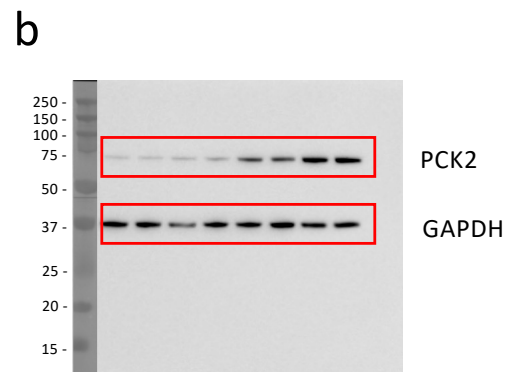


SUPPLEMENTARY FIGURE 9: EFFECT OF 3-MPA-MEDIATED CHEMICAL BLOCKADE OF PCK2'S CATALYTIC ACTIVITY ON KEY PHENOTYPIC PARAMETERS

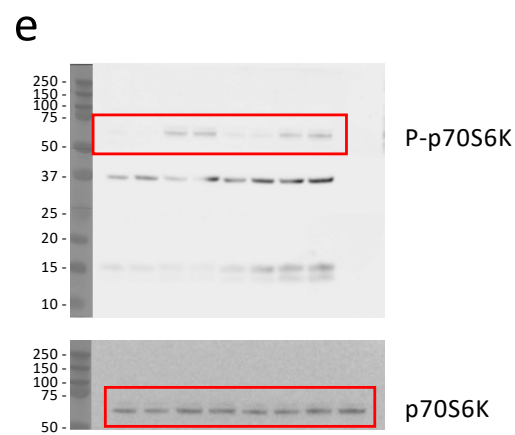
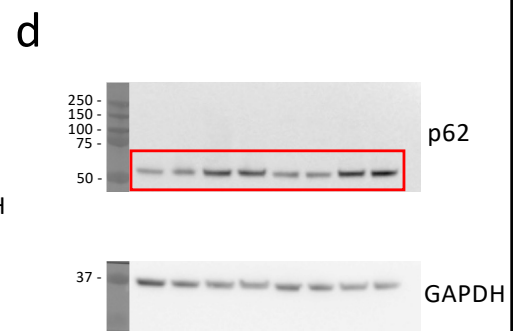
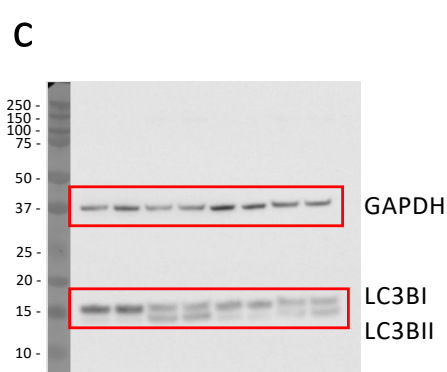
a-b, Densitometric quantifications (Western blots) of BiP (a) and ATF4 (b) protein levels, normalized to loading control (GAPDH), in control or 3-MPA (100 μ M)-treated ECs at the indicated glucose concentrations. Data are mean \pm s.e.m.; n=5. Statistics: one-way ANOVA; * $P<0.05$; ** $P<0.01$; *** $P<0.001$; ns, not significant. **c**, Representative immunofluorescence images of LAMP1 (green), proteostat (red), F-actin (white) and Hoechst (blue) staining in control (scramble; SCR), PCK2^{KD1} and 3-MPA-treated (100 μ M) ECs in 5.5 mM glucose (n=3). Panels on the right are single-channel zoom-ins of the boxed area in the merged images on the left. Scale bar 20 μ m. **d-f**, Effect of 3-MPA treatment (100 μ M) on proliferation (d), cell death (e) and wound healing (migration) (f) in ECs at 5.5 or 0 mM glucose. Data are mean \pm s.e.m.; n \geq 3. Statistics: one-way ANOVA; *** $P<0.001$; ns, not significant.

Figure S10 (part 1/3)

blots shown in Figure 1



blots shown in Figure 5



blots shown in Figure 6

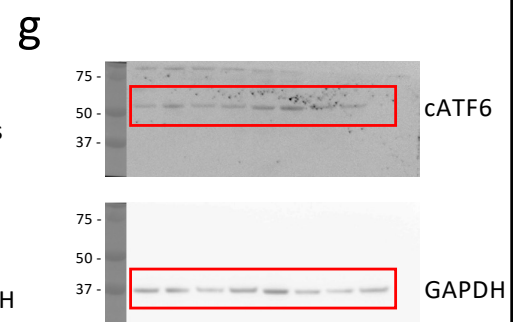
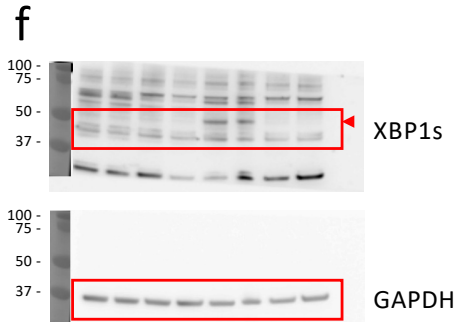
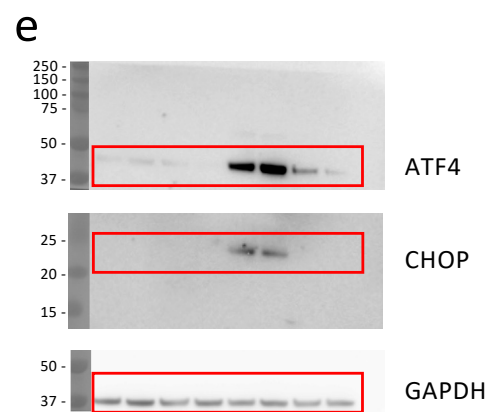
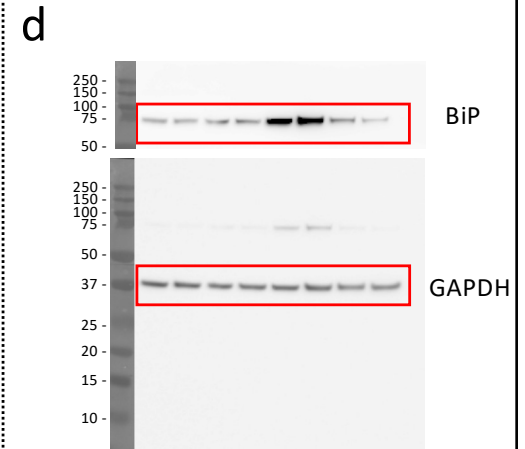
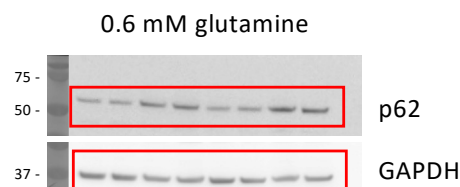
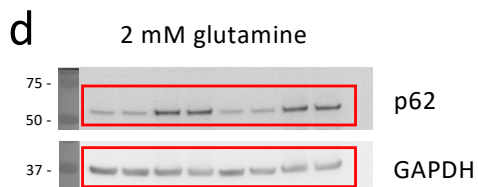
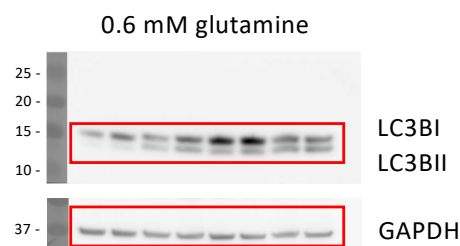
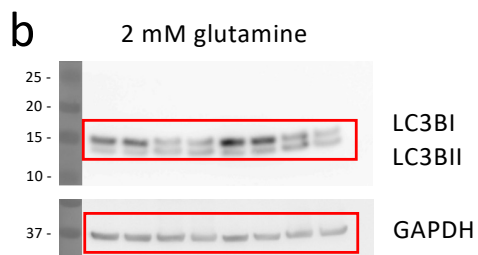


Figure S10 (part 2/3)

blots shown in Figure S1



blots shown in Figure S6



blots shown in Figure S7

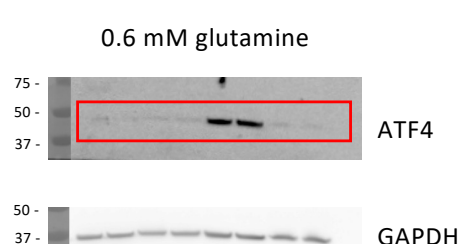
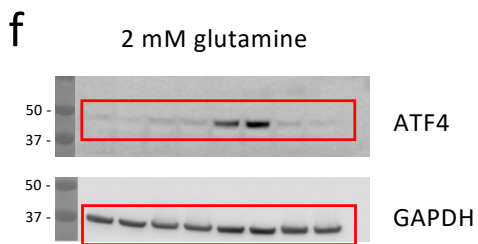
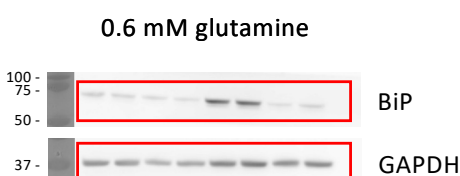
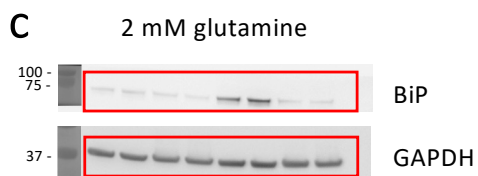
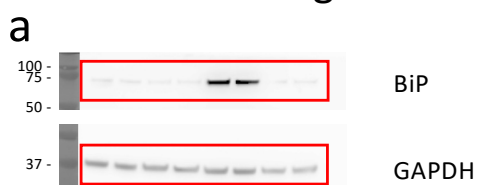


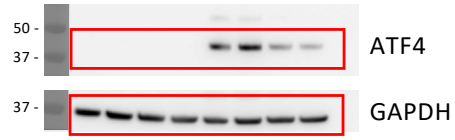
Figure S10 (part 3/3)

blots shown in Figure S8

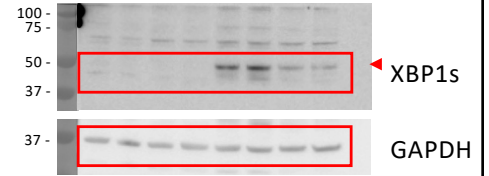
a



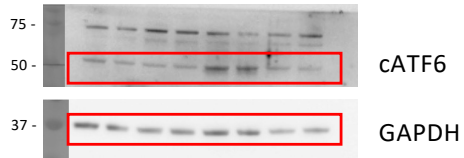
b



c



d



e



SUPPLEMENTARY FIGURE 10: UNCROPPED WESTERN BLOTS FOR DATA SHOWN IN MAIN AND SUPPLEMENTARY FIGURES.

Individual panels show the uncropped blots with size markers. Red boxes indicate the lanes shown in the figures. Depending on the expected band sizes, blots were cut appropriately to allow for immunoblotting of the respective proteins and loading controls. For space reasons supplementary figures are referred to as 'Figure S'.

SUPPLEMENTARY DATA 1: SOURCE DATA OF THE QUANTIFIED RESULTS OF THE MAIN FIGURES (enclosed excel file)